Covid-19 Detection by Wavelet Entropy and Cat Swarm Optimization

Wei Wang(✉)

Informatics Building, School of Informatics, University of Leicester, University Road, Leicester LE1 7RH, UK
ww152@leicester.ac.uk

Abstract. The rapid global spread of COVID-19 poses a huge threat to human security. Accurate and rapid diagnosis is essential to contain COVID-19, and an artificial intelligence-based classification model is an ideal solution to this problem. In this paper, we propose a method based on wavelet entropy and Cat Swarm Optimization to classify chest CT images for the diagnosis of COVID-19 and achieve the best performance among similar methods. The mean and standard deviation of sensitivity is 74.93 ± 2.12, specificity is 77.57 ± 2.25, precision is 76.99 ± 1.79, accuracy is 76.25 ± 1.49, F1-score is 75.93 ± 1.53, Matthews correlation coefficient is 52.54 ± 2.97, Feature Mutual Information is 75.94 ± 1.53.

Keywords: COVID-19 · Wavelet entropy · Cat Swarm Optimization · Feedforward Neural Network · K-fold cross-validation

1 Introduction

Since the novel new coronavirus was first discovered in Wuhan, China in 2019, the virus has rapidly spread to various countries worldwide, causing massive deaths. The World Health Organization (WHO) has named the virus Severe Acute Respiratory Syndrome Coronavirus-2 (SARS-CoV-2) [1] and defined the global pandemic it caused (COVID-19) as a Public Health Emergencies of International Concern (PHEIC) [2].

In addition to the extremely high transmission rate of SARS-CoV-2, the more complex diagnostic identification is a significant reason for the rapid spread. The most recognised method for the detection of COVID-19 is the reverse-transcription polymerase chain reaction (RT-PCR). Although RT-PCR offers high diagnostic accuracy, it has the disadvantage of being time-consuming (up to two days) and has a high false-negative rate [3]. The asymptomatic patients (who are not obviously symptomatic but are still infectious) significantly hampered rapid identification and monitoring of COVID-19 [4]. The search for a rapid and accurate COVID-19 test is an urgent task in the fight against the epidemic.

Medical studies have confirmed that the features in chest CT images can effectively reflect the focal status of COVID-19. The chest CT images combined with epidemiological and laboratory tests effectively assess COVID-19 [5]. However, manual-based

S. Wang et al. (Eds.): IoTCare 2021, LNICST 415, pp. 479–487, 2022.
https://doi.org/10.1007/978-3-030-94182-6_38

examinations are labour-intensive and time-consuming, and artificial intelligence is ideal for this process.

Lu, Z. (2016) [6] used a radial basis function (RBF) based method to detect brain disease, which can also be generalised to COVID-19 detection. Yao, X. et al. (2020) [7] proposed an experiment using wavelet entropy (WE) and biogeography-based optimisation (BBO) based method to classify chest CT images to diagnose COVID-19 and achieved good performance. Chen, Y. (2020) [8] proposed a method based on support vector machine (SVM) and grey-level co-occurrence matrix (GLCM) to classify chest CT images of heath people and COVID-19 patients.

This paper proposes a WE and Cat Swarm Optimization (CSO) based method for COVID-19 identification and obtains the highest performance among similar methods. The main contributions of the paper are: (i) The first classification model to combine WE and CSO. (ii) The best performance in WE based COVID-19 diagnostic approaches.

2 Dataset

The experiment used a dataset of COVID-19 CT images from the Fourth People's Hospital in Huai'an, China, taken from 66 as COVID-19-infected and 66 healthy individuals, for a total of 132 subjects. Each data sample consisted of CT images of the lungs and the corresponding accounting test results. These subjects had a maximum age of 24 years and a minimum age of 91 years and comprised 77 males and 55 females. The selection and labelling of the dataset performed by two specialist radiologists who simultaneously identified and labelled the CT images uploaded to the Picture Archiving and Communication System (PASC), selecting 1–4 CT images with suitable lesion identification for each subject infected with COVID-19. The portion of the dataset for healthy subjects was obtained from a random sample of 159 healthy subjects with physical examination results. The Fig. 1 show two image samples of the dataset.

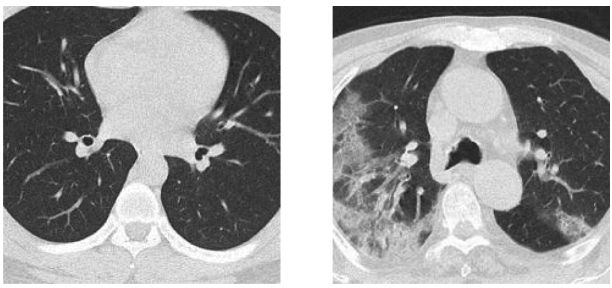

Fig. 1. CT Image sample of Health Control (*left*) and COVID Patient (*right*).

3 Methodology

3.1 Wavelet Entropy

The experiment uses the Discrete Wavelet Transform (DWT) as a feature extraction method, a popular method for signal analysis [9]. DWT inherits the main ideas of the Fourier Transform and addressed the disadvantages of the Fourier Transform for processing unstable signals by replacing the wireless length trigonometric basis with a finite length decaying wavelet basis while preserving the time and frequency information of the signal [10]. The Fourier Transform is defined as Eq. (1) and the DWT is defined as Eq. (2).

$$F(\omega) = \int_{-\infty}^{\infty} f(t) e^{-i\omega t} dt \tag{1}$$

where ω refers to frequency, t refers to time.

$$W(a, \tau) = \frac{1}{\sqrt{a}} \int_{-\infty}^{\infty} f(t) \psi * \left(\frac{t - \tau}{a} \right) dt \tag{2}$$

where a represents scale, τ represents translation, ψ represents parent wavelet function, and t represents time.

DWT can use the multi-scale nature of orthogonal wavelets to effectively decompose images at different scales (resolutions) [11] and retain as much image information as possible. Image contours are preserved in large-scale spaces, and image details are preserved in the small-scale space. This property can effectively improve the recognition of small lesions in medical images. However, too much image information requires a large amount of space and computational cost [12]. Therefore, we introduced entropy to reduce the dimensionality of the dataset while retaining as much valid information as possible. Entropy is a stochastic statistic that can be approximated from the grey-scale probability histogram of an image. The Eq. (3) defines the entropy.

$$S(\alpha) = -\sum\nolimits_i P(\alpha_i) log_b P(\alpha_i) \tag{3}$$

where α refers to grey levels and P is the probabilities of grey levels [13].

The original image signal is used as input, and after the first level wavelet decomposition, we can obtain four matrices, one low-frequency component (LL1) and three high-frequency components (HL1, LH1, HH1). The second level wavelet decomposition of the resulting low-frequency components yields a low-frequency component (LL2) and three new high-frequency components (HL1, LH1, HH1). Repeat the above procedure after a total of n matrix decompositions, one low-frequency component (LLn), and n high-frequency components (HL1, LH1, HH1,…, HLn, LHn, HHn) are finally obtained. The entropy is then extracted from these components represented in matrix form [14], allowing for a vector of entropy with a feature reduction to n+1 values [15]. These values can be used as input to the neural network [16]. The Fig. 2 shows a brief demonstration of the whole process.

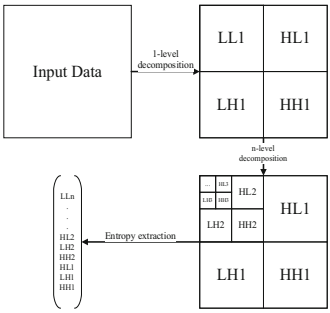

Fig. 2. DWT multi-level decomposition

3.2 Feedforward Neural Network

A feed-forward neural network (FNN) is a simple type of artificial neural network that is often used as a classifier for pattern classification [17]. FNN mainly consist of an input layer, one (superficial network) or more (deep network) hidden layers and an output layer. Inside the FNN, each layer (except the output layer) connected to the next [18], and parameters are propagated singularly from the input layer through the hidden layer to the output layer. The Fig. 3 illustrates the basic structure of an FNN. Deep FNN [19, 20] is our future research direction.

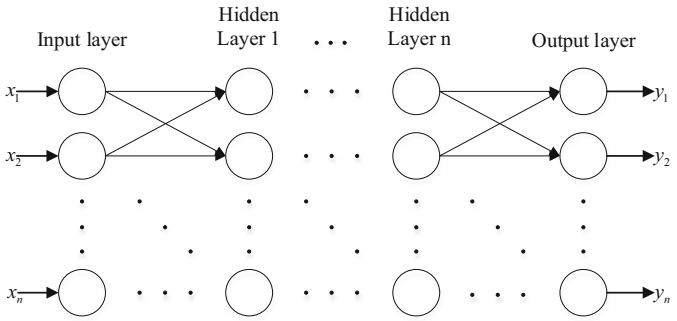

Fig. 3. The basic structure of Feedforward Neural Network

3.3 Cat Swarm Optimization

CSO is an algorithm that optimises values by mimicking the behaviour of cats in nature [21], using a predetermined ratio (MR) to determine the number of agents (cats) in both seeking and tracking modes [22]. There are four elements defined for the seeking mode:

- Seeking Memory Pool (SMP) defines the size of seeking memory for each cat.
- Seeking Range of the selected Dimension (SRD) provides the boundary conditions for change.

- Counts of Dimensions to Change (CDC) indicate the number of dimensions to change [23].
- Self-Position Considering (SPC) determines whether the current position of the cat is used as a seeking memory candidate coordinate.

Unlike the slowness of the seeking mode, the tracking mode simulates a cat's fast pursuit of a target, for a D-dimension space, the velocities of cats are represented as $V_i = (V_{i1}, V_{i2}, \cdots, V_{iD})$. The main idea of CSO is to solve the optimisation problem by uniting two sets of cats [24], as shown in Fig. 4.

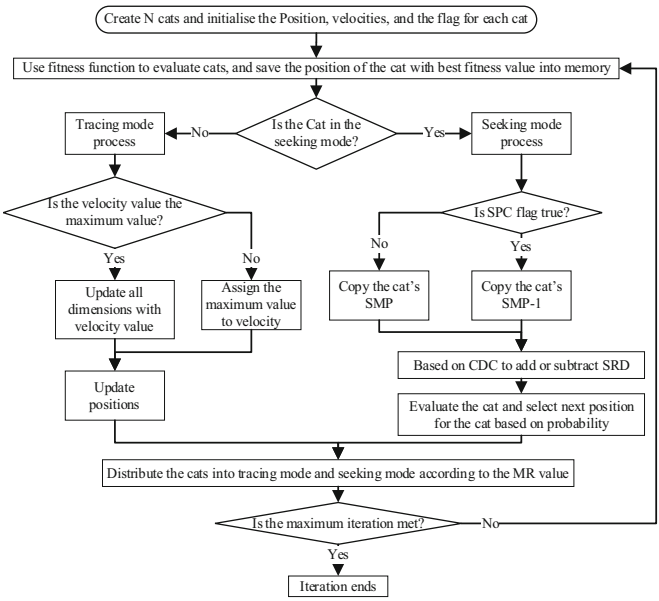

Fig. 4. Flowchart of the Cat Swarm Optimization algorithm

3.4 K-fold Cross Validation

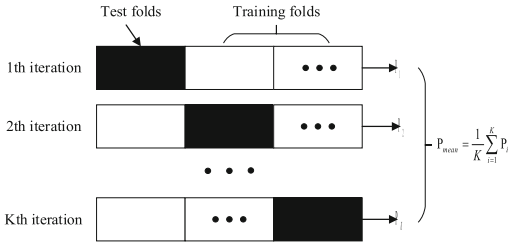

Fig. 5. Illustration of K-fold cross validation

K-fold cross validation is a data set partitioning method that effectively addresses the adverse effects of too small a data set [25]. The value of K is predetermined based on the size of the data set [26]. The K value affects the performance of the final model, with the larger value of K, the smaller the size of the dataset, but the more computational resources required [27, 28]. The Fig. 5 illustrates the K-fold cross validation.

4 Experiment Results and Discussions

4.1 WE Results

The Fig. 6 illustrates a four-level discrete wavelet transform sample image. The three most giant blocks in the image are the three high-frequency components produced by the first-level wavelet transform. Similarly, the high-frequency components produced by the second, third and fourth level wavelet transform could be found in the image. The low-frequency components of the first three wavelet transform are used for the next level wavelet transform. The only low-frequency component left is produced by the fourth level wavelet transform, which is the block at the top left corner in the image.

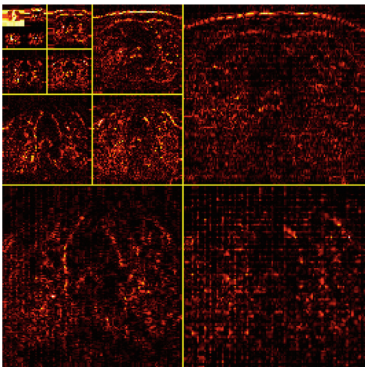

Fig. 6. Four-level discrete wavelet transform sample image.

4.2 Statistical Results

The experiments used 10-fold cross-validation [29] to ensure efficient dataset using and the results are unbiased [30]. The detail results of 10 times running are listed in the Table 1, in which the mean and standard deviation (Mean + SD) of sensitivity (Sen) is 74.93 ± 2.12, specificity (Spc) is 77.57 ± 2.25, precision (Prc) is 76.99 ± 1.79, accuracy (Acc) is 76.25 ± 1.49, F1-score (F1) is 75.93 ± 1.53, Matthews correlation coefficient (MCC) is 52.54 ± 2.97, Feature Mutual Information (FMI) is 75.94 ± 1.53.

Table 1. 10 runs of 10-fold cross-validation

Run	Sen	Spc	Prc	Acc	F1	MCC	FMI
1	72.97	78.38	77.14	75.68	75.00	51.43	75.03
2	77.70	76.35	76.67	77.03	77.18	54.06	77.18
3	74.32	79.73	78.57	77.03	76.39	54.13	76.42
4	73.65	79.05	77.86	76.35	75.69	52.78	75.72
5	78.38	81.08	80.56	79.73	79.45	59.48	79.46
6	74.32	76.35	75.86	75.34	75.09	50.69	75.09
7	72.97	76.35	75.52	74.66	74.23	49.35	74.24
8	77.70	73.65	74.68	75.68	76.16	51.39	76.17
9	73.65	79.05	77.86	76.35	75.69	52.78	75.72
10	73.65	75.68	75.17	74.66	74.40	49.33	74.41
Mean + SD	74.93 ± 2.12	77.57 ± 2.25	76.99 ± 1.79	76.25 ± 1.49	75.93 ± 1.53	52.54 ± 2.97	75.94 ± 1.53

4.3 Comparison to State-of-the-Art Approaches

The result of the research has achieved a better performance than other state-of-art approaches in multiple metrices. The detailed comparison in all metrices is summarised in the Table 2, which validates our approach as a viable and promising approach in the field of medical image classification.

Table 2. Performance comparison to other methods

Method	Sen	Spc	Prc	Acc	F1	MCC	FMI
RBFNN [6]	66.89 ± 2.43	75.47 ± 2.53	73.23 ± 1.48	71.18 ± 0.80	69.88 ± 1.08	42.56 ± 1.61	69.97 ± 1.04
WE-BBO [7]	72.97 ± 2.96	74.93 ± 2.39	74.48 ± 1.34	73.95 ± 0.98	73.66 ± 0.98	47.99 ± 2.00	73.66 ± 1.33
GLCM-SVM [8]	72.03 ± 2.94	78.04 ± 1.72	76.66 ± 1.07	75.03 ± 1.12	74.24 ± 1.57	50.20 ± 2.17	74.29 ± 1.53
Ours	74.93 ± 2.12	77.57 ± 2.25	76.99 ± 1.79	76.25 ± 1.49	75.93 ± 1.53	52.54 ± 2.97	75.94 ± 1.53

5 Conclusions

The potential of artificial intelligence to classify features in CT images cannot be ignored, and the rapid and accurate diagnosis it can bring is of considerable importance to the

medical field. The performance of our proposed method based on wavelet entropy and cat swarm optimisation also confirms the feasibility of a time-frequency based classification method for the COVID-19 CT image classification task.

References

1. Hotez, P.J., Fenwick, A., Molyneux, D.: The new COVID-19 poor and the neglected tropical diseases resurgence. Infect. Dis. Poverty **10**(1), 10 (2021)
2. Yuki, K., Fujiogi, M., Koutsogiannaki, S.: COVID-19 pathophysiology: a review. Clin. Immunol. **215**, 108427 (2020)
3. Fang, Y., et al.: Sensitivity of chest CT for COVID-19: comparison to RT-PCR. Radiology **296**(2), E115–E117 (2020)
4. Meng, H., et al.: CT imaging and clinical course of asymptomatic cases with COVID-19 pneumonia at admission in Wuhan, China. J. Infect. **81**(1), e33–e39 (2020)
5. Zhao, X., et al.: The characteristics and clinical value of chest CT images of novel coronavirus pneumonia. Clin. Radiol. **75**(5), 335–340 (2020)
6. Lu, Z.: A pathological brain detection system based on radial basis function neural network. J. Med. Imaging Health Inf. **6**(5), 1218–1222 (2016)
7. Yao, X., Han, J.: COVID-19 detection via wavelet entropy and biogeography-based optimization. In: Santosh, K.C., Joshi, A. (eds.) COVID-19: Prediction, Decision-Making, and its Impacts. LNDECT, vol. 60, pp. 69–76. Springer, Singapore (2021). https://doi.org/10.1007/978-981-15-9682-7_8
8. Chen, Y.: Covid-19 classification based on gray-level co-occurrence matrix and support vector machine. In: Santosh, K.C., Joshi, A. (eds.) COVID-19: Prediction, Decision-Making, and its Impacts. LNDECT, vol. 60, pp. 47–55. Springer, Singapore (2021). https://doi.org/10.1007/978-981-15-9682-7_6
9. Guido, R.C.: Nearly symmetric orthogonal wavelets for time-frequency-shape joint analysis: introducing the discrete shapelet transform's third generation (DST-III) for nonlinear signal analysis. Commun. Nonlinear Sci. Numer. Simul. **97**, 105685 (2021). Article ID 105685
10. Saritha, M., et al.: Classification of MRI brain images using combined wavelet entropy based spider web plots and probabilistic neural network. Pattern Recogn. Lett. **34**(16), 2151–2156 (2013)
11. Chui, C.K., et al.: Wavelet thresholding for recovery of active sub-signals of a composite signal from its discrete samples. Appl. Comput. Harmon. Anal. **52**, 1–24 (2021)
12. El-Dahshan, E.-S.A., et al.: Hybrid intelligent techniques for MRI brain images classification. Digit. Sig. Process. **20**(2), 433–441 (2010)
13. Yildiz, A., et al.: Application of adaptive neuro-fuzzy inference system for vigilance level estimation by using wavelet-entropy feature extraction. Exp. Syst. Appl. **36**(4), 7390–7399 (2009)
14. Phillips, P.: Pathological brain detection in magnetic resonance imaging scanning by wavelet entropy and hybridization of biogeography-based optimization and particle swarm optimization. Prog. Electromagnet. Res. **152**, 41–58 (2015)
15. Yang, M., Automatic brain tumor detection in MRI Scanning by wavelet entropy. J. Am. Geriatr. Soc. **64**(S2), S349–S349 (2016). Article ID 349
16. Phillips, P.: Intelligent facial emotion recognition based on stationary wavelet entropy and Jaya algorithm. Neurocomputing **272**, 668–676 (2018)
17. Nakamura-Zimmerer, T., et al.: QRnet: optimal regulator design with LQR-augmented neural networks. IEEE Control Syst. Lett. **5**(4), 1303–1308 (2021)

18. Wang, S.-H., Muhammad, K., Hong, J., Sangaiah, A.K., Zhang, Y.-D.: Alcoholism identification via convolutional neural network based on parametric ReLU, dropout, and batch normalization. Neural Comput. Appl. **32**(3), 665–680 (2018)
19. Wang, S.-H., Zhang, Y.-D.: DenseNet-201-based deep neural network with composite learning factor and precomputation for multiple sclerosis classification. ACM Trans. Multimedia Comput. Commun. Appl. **16**(2s), 1–19 (2020). Article 60
20. Alcaraz, J.C., Moghaddamnia, S., Peissig, J.: Efficiency of deep neural networks for joint angle modeling in digital gait assessment. EURASIP J. Adv. Sig. Process. **2021**(1), 1–20 (2021). Article ID 10
21. Suresh, M., Sam, I.S.: Exponential fractional cat swarm optimization for video steganography. Multimedia Tools Appl. **80**(9), 13253–13270 (2021). https://doi.org/10.1007/s11042-020-10395-6
22. Wang, S.-H., Yang, W., Dong, Z., Phillips, P., Zhang, Y.-D.: Facial emotion recognition via discrete wavelet transform, principal component analysis, and cat swarm optimization. In: Sun, Yi., Lu, H., Zhang, L., Yang, J., Huang, H. (eds.) IScIDE 2017. LNCS, vol. 10559, pp. 203–214. Springer, Cham (2017). https://doi.org/10.1007/978-3-319-67777-4_18
23. Zhang, Y.-D., Sui, Y., Sun, J., Zhao, G., Qian, P.: Cat Swarm Optimization applied to alcohol use disorder identification. Multimedia Tools Appl. **77**(17), 22875–22896 (2018)
24. Saha, S.K., et al.: Cat swarm optimization algorithm for optimal linear phase FIR filter design. ISA Trans. **52**(6), 781–794 (2013)
25. Akbari, H., Sadiq, M.T., Rehman, A.U.: Classification of normal and depressed EEG signals based on centered correntropy of rhythms in empirical wavelet transform domain. Health Inf. Sci. Syst. **9**(1), 1–15 (2021). Article ID 9
26. Wang, S.-H.: COVID-19 classification by CCSHNet with deep fusion using transfer learning and discriminant correlation analysis. Inf. Fus. **68**, 131–148 (2021)
27. Wang, S.-H., Zhang, Y., Cheng, X., Zhang, X., Zhang, Y.-D.: PSSPNN: PatchShuffle stochastic pooling neural network for an explainable diagnosis of COVID-19 with multiple-way data augmentation. Comput. Math. Meth. Med. **2021**, 1–18 (2021). Article ID 6633755
28. Rajapandy, M., Anbarasu, A.: An improved unsupervised learning approach for potential human microRNA–disease association inference using cluster knowledge. Netw. Model. Anal. Health Inf. Bioinf. **10**(1), 1–16 (2021). Article ID 21
29. Bodaghi, S., et al.: Regularization of a nonlinear inverse problem by discrete mollification method. Comput. Meth. Differ. Eqn. **9**(1), 313–326 (2021)
30. Govindaraj, V.: Explainable diagnosis of secondary pulmonary tuberculosis by graph rank-based average pooling neural network. J. Ambient Intell. Humanized Comput. (2021). https://doi.org/10.1007/s12652-021-02998-0